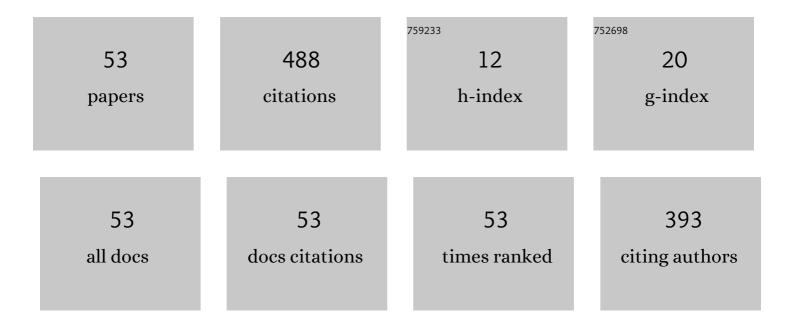
Bin Tang

List of Publications by Year in descending order

Source: https://exaly.com/author-pdf/1293118/publications.pdf Version: 2024-02-01



RIN TANC

#	Article	IF	CITATIONS
1	Aliovalent Doping Engineering for A- and B-Sites with Multiple Regulatory Mechanisms: A Strategy to Improve Energy Storage Properties of Sr _{0.7} Bi _{0.2} TiO ₃ -Based Lead-Free Relaxor Ferroelectric Ceramics. ACS Applied Materials & Interfaces, 2021, 13, 24833-24855.	8.0	79
2	Structure and microwave dielectric properties of the Li _{2/3(1â^'<i>x</i>)} Sn _{1/3(1â^'<i>x</i>)} Mg _{<i>x</i>} O systems (<i>xÂ</i> =Â0â€4/7). Journal of the American Ceramic Society, 2018, 101, 252-264.	3.8	59
3	A new lowâ€firing and highâ€Q microwave dielectric ceramic Li ₉ Zr ₃ NbO ₁₃ . Journal of the American Ceramic Society, 2018, 101, 2202-2207.	3.8	22
4	Ferroelectric-Relaxor Crossover and Energy Storage Properties in Sr ₂ NaNb ₅ O ₁₅ Based Tungsten Bronze Ceramics. ACS Applied Materials & Interfaces, 2022, 14, 9318-9329.	8.0	22
5	Relationships between Sn substitution for Ti and microwave dielectric properties of Mg2(Ti1â^'xSnx)O4 ceramics system. Journal of Materials Science: Materials in Electronics, 2015, 26, 571-577.	2.2	21
6	Effects of perfluorooctyltriethoxysilane coupling agent on the properties of silica filled PTFE composites. Journal of Materials Science: Materials in Electronics, 2017, 28, 8810-8817.	2.2	19
7	Influence of SiO2 Addition on Properties of PTFE/TiO2 Microwave Composites. Journal of Electronic Materials, 2018, 47, 633-640.	2.2	18
8	Effect of sintering temperature on the crystallization behavior and properties of silica filled PTFE composites. Journal of Materials Science: Materials in Electronics, 2016, 27, 13288-13293.	2.2	17
9	Microwave dielectric properties of (1â€ <i>x</i>)Ba _{3.75} Nd _{9.5} Cr _{0.25} Nb _{0.25} Ti _{17.5} ceramics. Journal of the American Ceramic Society, 2017, 100, 4058-4065.	O 3.s ub>5	4< ‡s ub>‰
10	Lowâ€fire processing and microwave dielectric properties of LB glassâ€doped Ba _{3.75} Nd _{9.5} Ti _{17.5} (Cr _{0.5} Nb _{0.5}) _{0.5ceramic. Journal of the American Ceramic Society, 2021, 104, 1726-1739.}	> @ 8sub>	5 46 /sub>
11	Effects of compound coupling agents on the properties of PTFE/SiO2 microwave composites. Journal of Materials Science: Materials in Electronics, 2017, 28, 3356-3363.	2.2	15
12	Dependence of microwave dielectric properties on site substitution in Ba3.75Nd9.5Ti18O54 ceramic. Journal of Materials Science: Materials in Electronics, 2016, 27, 10951-10957.	2.2	14
13	Different Additives Doped Ca–Nd–Ti Microwave Dielectric Ceramics with Distorted Oxygen Octahedrons and High <i>Q</i> × <i>f</i> Value. ACS Omega, 2018, 3, 11033-11040.	3.5	12
14	Effects of (Na1/2Nd1/2)TiO3 on the microstructure and microwave dielectric properties of PTFE/ceramic composites. Journal of Materials Science: Materials in Electronics, 2018, 29, 20680-20687.	2.2	9
15	Microwave dielectric properties of Li ₂ 0– <i>x</i> MgO–ZnO–B ₂ 0 ₃ –SiO ₂ glass-ceramic (<i>x</i> = 30–50 wt.%). Journal of the Ceramic Society of Japan, 2018, 126, 163-169.	31.1	9
16	Researches on silane coupling agent treated AlN ceramic powder and fabrication of AlN/PTFE composites for microwave substrate applications. Journal of Materials Science: Materials in Electronics, 2019, 30, 20189-20197.	2.2	9
17	Microwave Dielectric Properties of Aluminum‧ubstituted Ba _{6â^'3<i>x</i>} Nd _{8+2<i>x</i>} Ti ₁₈ O ₅₄ Ceramics. International Journal of Applied Ceramic Technology, 2016, 13, 564-568.	2.1	8
18	Preparation, characterization and properties of FEP modified PTFE/glass fiber composites for microwave circuit application. Journal of Materials Science: Materials in Electronics, 2017, 28, 6015-6021.	2.2	8

Bin Tang

#	Article	IF	CITATIONS
19	Iterative High-Accuracy Parameter Estimation of Uncooperative OFDM-LFM Radar Signals Based on FrFT and Fractional Autocorrelation Interpolation. Sensors, 2018, 18, 3550.	3.8	8
20	Automatic LPI Radar Signal Sensing Method Using Visibility Graphs. IEEE Access, 2020, 8, 159650-159660.	4.2	8
21	Novel Unconventional-Active-Jamming Recognition Method for Wideband Radars Based on Visibility Graphs. Sensors, 2019, 19, 2344.	3.8	7
22	Deep learning-based specific emitter identification using integral bispectrum and the slice of ambiguity function. Signal, Image and Video Processing, 2022, 16, 2009-2017.	2.7	7
23	Effects of Zr-Substitution on Microwave Dielectric Properties of Na0.5Nd0.2Sm0.3Ti1â^x Zr x O3 Ceramics (xÂ=Â0.00Ââ^¼Â0.30). Journal of Electronic Materials, 2016, 45, 5198-5205.	2.2	6
24	Radar ECCM based on phase-aid distributed compressive sensing. Signal, Image and Video Processing, 2018, 12, 1497-1504.	2.7	6
25	Research on hydrophobicity treatment of aluminum nitride powder and the fabrication and characterization of AlN/PTFE composite substrates. Journal of Materials Science: Materials in Electronics, 2018, 29, 14890-14896.	2.2	6
26	Radar Antenna Scan Pattern Intelligent Recognition Using Visibility Graph. IEEE Access, 2019, 7, 175628-175641.	4.2	6
27	Tunable valleytronics with symmetry-retaining high polarization degree in SnSxSe1â^'x model system. Applied Physics Letters, 2020, 116, 061105.	3.3	6
28	A new niobate-based CaO–2CuO–Nb2O5 microwave dielectric ceramic composite for LTCC applications. Journal of Materials Science: Materials in Electronics, 2018, 29, 4533-4537.	2.2	5
29	Deceptive multiple false targets jamming recognition for linear frequency modulation radars. Journal of Engineering, 2019, 2019, 7690-7694.	1.1	5
30	Chemically Modulating the Twist Rate of Helical van der Waals Crystals. Chemistry of Materials, 2020, 32, 299-307.	6.7	5
31	Wideband Spectrum Sensing via Derived Correlation Matrix Completion Based on Generalized Coprime Sampling. IEEE Access, 2019, 7, 117403-117410.	4.2	4
32	Influence of Li2O–MgO–ZnO–B2O3–SiO2 glass doping on the microwave dielectric properties and sintering temperature of Li3Mg2NbO6 ceramics. Journal of Materials Science: Materials in Electronics, 2020, 31, 17029-17035.	2.2	4
33	Key Parameter Estimation for Pulse Radar Signal Intercepted by Non-Cooperative Nyquist Folding Receiver. IEICE Transactions on Fundamentals of Electronics, Communications and Computer Sciences, 2018, E101.A, 1934-1939.	0.3	4
34	Impacts of Al ₂ O ₃ Doping on Microstructure, Phase Constitution and Microwave Dielectric Properties of Ca _{0.61} Nd _{0.26} TiO ₃ Ceramics. Transactions of the Indian Ceramic Society, 2017, 76, 97-101.	1.0	3
35	A Switched-Element System Based Direction of Arrival (DOA) Estimation Method for Un-Cooperative Wideband Orthogonal Frequency Division Multi Linear Frequency Modulation (OFDM-LFM) Radar Signals. Sensors, 2019, 19, 132.	3.8	3
36	Performance Analysis of Data Transmission for Joint Radar and Communication Systems. Mathematical Problems in Engineering, 2021, 2021, 1-14.	1.1	3

Bin Tang

#	Article	IF	CITATIONS
37	Low-temperature sintering kinetics and dielectric properties of Ba5Nb4O15 with B2O3–SiO2 glass. Journal of Materials Science: Materials in Electronics, 2021, 32, 8716-8724.	2.2	3
38	Deep learning-based LPI radar signals analysis and identification using a Nyquist Folding Receiver architecture. Defence Technology, 2023, 19, 196-209.	4.2	3
39	A Temperature-Insensitive Ba3.75Nd9.5Ti17.5(Cr0.5Nb0.5)0.5O54 Microwave Dielectric Ceramic by Bi3+ Substitution. Journal of Electronic Materials, 2017, 46, 1230-1234.	2.2	2
40	A Dynamic Conflict Analysis Method for EW Effectiveness Evaluation Based on Conditional State Space. Electronics (Switzerland), 2021, 10, 24.	3.1	2
41	Tailoring sintering kinetics and dielectric properties of Li2SiO3 ceramics by CaO–B2O3–SiO2 glass dopant for LTCC substrate applications. Journal of Materials Science: Materials in Electronics, 2022, 33, 4043-4050.	2.2	2
42	Radar Signal Sorting Using Combined Residual and Recurrent Neural Network (CRRNN). , 2021, , .		2
43	Undersampling channelized receiver using principle of signal matched-phase. IEICE Electronics Express, 2012, 9, 213-219.	0.8	1
44	Iterative Interpolar based Switched Element Direction Finding for Wideband Linear Frequency Modulated Signals. , 2019, , .		1
45	Detection of Unresolved Targets for Wideband Monopulse Radar. Sensors, 2019, 19, 1084.	3.8	1
46	Microwave dielectric properties and low-fire processing of Ca0.244Li0.3Nd0.404Ti0.96Al0.02Nb0.02O3 ceramics doped with BZLBS. Journal of Materials Science: Materials in Electronics, 0, , .	2.2	1
47	Passive Localization Algorithm for Spaceborne SAR Using NYFR and Sparse Bayesian Learning. IEICE Transactions on Fundamentals of Electronics, Communications and Computer Sciences, 2019, E102.A, 581-585.	0.3	0
48	Robust design and evaluation of phase codes for radar performance optimization with a finite alphabet constraint. Electronics Letters, 2021, 57, 415-418.	1.0	0
49	Non-Cooperative Detection Method of MIMO-LFM Signals with FRFT Based on Entropy of Slice. IEICE Transactions on Fundamentals of Electronics, Communications and Computer Sciences, 2018, E101.A, 1940-1943.	0.3	0
50	A Detection Method of Multi-Sensor for Radar Countermeasure Network. , 2020, , .		0
51	An Approach of LPI Radar Signal Detection Based on Visibility Graph. , 2020, , .		0
52	KL divergence Based Objective State Selection Method for EW Conflict. , 2021, , .		0
53	Complex (Mg1/3Ta2/3)4+ ionic substitution on the phase structure and microwave dielectric properties of wolframite MgZr1â^x(Mg1/3Ta2/3)xNb2O8 (0 â‰ 8 €‰x â‰ 8 €‰0.08) ceramics. Journal of Materia	als S øience:	: 0

Materials in Electronics, 0, , 1.